PREPRINT UCRL- 80132 Rev. I

CONF-771136--1

Lawrence Livermore Laboratory

Confirmation of Radiation Pressure Effects in Laser-Plasma Interactions

D. T. Attwood, D. W. Sweeney, J. M. Auerbach and P. H. Y. Lee

October, 1977

This paper was prepared for submission to the 1977 Annual American Physical Society Meeting, Atlanta, Georgia, November 7-11, 1977 and also for submission to the Journal of Physical Review Letters

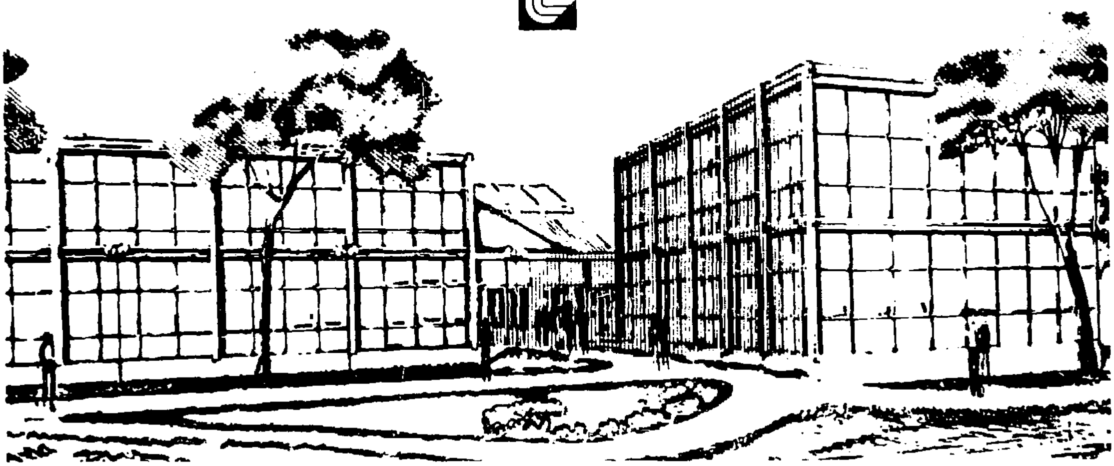

Confirmation of Radiation Pressure Effects In Laser-Plasma Interactions*

D. T. Attwood, D. W. Sweeney, J. M. Auerbach and P. H. Y. Lee

Lawrence Livermore Laboratory, University of California
Livermore, CA 94550

Abstract

Interferometric data resolved to 1μm and 15 psec confirms the dominant role of radiation pressure during high intensity laser-plasma interactions. Specifically observed manifestations include electron density profiles steepened to 1μm scale length, clearly defined upper and lower density shelves, and small and large scale deformation of transverse isodensity surfaces.

*Work peformed under the auspices of the U.S. Department of Energy under Contract No. W-7405-Eng-48.

Prompted by current interest in laser induced fusion, a number of papers have recently been published concerning the interaction of intense laser light with the plasma surrounding irradiated targets, and in particular the significant role of radiation pressure in both large and small scale deformation of the critical surface. The literature describes optical absorption and scattering in the presence of self-steepened electron density profiles,[1] density cavities and generalized modulation of the critical surface.[2] Reports to date have been limited primarily to theoretical and computational studies because of the stringent experimental requirements, viz., space-time resolution of microns (μm) and picoseconds (psec) are essential for measurements during irradiation. Supporting experimental work of an indirect nature[3], and on larger space-time scales has appeared.[4] The collective thrust of these papers is that radiation pressure modifies and deforms the critical surface when the energy density of the incident radiation is comparable to the thermal energy density of the plasma, and that these modifications in turn affect the absorption and transport of energy. In particular, it is predicted that these effects enhance the role of resonance absorption while reducing that of parametric processes, which require shallow axial gradients.[5] In this paper we present the first interferometric data with sufficient space-time resolution, 1 micron and 15 psec, to directly confirm the presence of profile steepening, cavity formation, and transverse rippling of the critical surface <u>during</u> irradiation by high intensity Nd-laser pulses.

The interaction experiments were performed at 1.06 μm wavelength with one beam of Livermore's Janus laser facility,[6] operating in this case with nominally 0.5 to 5 joule, 30 psec FWHM pulses, and f/10 focusing optics. Laser prepulse was measured with a threshold of 10 μJ. Targets consisted of 40 μm diameter SiO_2 glass microballoons, and 70-300 μm diameter glass and parylene disks. Electron temperatures, as deduced from a space-time integrated x-ray k-edge filter technique[7], ranged from 0.7 to 1 keV in these experiments.

Electron densities were measured interferometrically with a double exposure holographic technique[8] employing corrected f/2.5 optics and a 2660 Å probe pulse of several microjoules energy and 15 psec duration. The probe pulse was split from the main laser pulse just after the switchout, and then separately amplified, filtered and shaped. Breakup of the probe beam was avoided by maintaining the breakup integral below a value of 0.5. Frequency conversion was accomplished in successive KDP and ADP frequency doubling crystals. Conversion efficiency was set at a modest level to maximize pulse shortening.[9] Small target diameters were chosen to minimize the deleterious effects of probe beam refraction during passage through the strong axial gradient density field.[8] The probe pulse was synchronized with the 1.06 μm heating pulse to an accuracy of approximately 10 psec by streak photography.

A sample interferogram, obtained within 10 psec of peak intensity, is shown in Fig. 1a for a 41 μm diameter, 0.6 μm thick glass microshell. Peak intensity for this experiment was approximately 3×10^{14} W/cm^2. A silhouette of the original ball is overlaid for reference. Abel inverted electron densities[10] are shown in Fig. 1b for a transverse plane 4 μm from the original target surface. The 21 μm transverse scale is significant in that refractive limitations of the probing technique demand that this distance be no larger if critical electron density (10^{21} e/cc) is to be achieved. Densities along the symmetry (irradiation) axis are shown in Fig. 1c, along with typical error bars. Each point is obtained from the axial value in a plot similar to 1b. A three line best fit is included for comparison with theory. The measured 1.6 μm axial scale length in the critical region is undoubtedly larger than predicted values because of our 1 μm spatial resolution and departures from cylindrical symmetry.

For this particular experiment we estimate the ratio of electron quiver to thermal velocity to be $V_o/V_{th} \simeq 0.3$. Lee et al.[1], using a 1D isothermal model, predict upper and lower electron density shelf values of approximately 1.2 and 0.6 n_c for these conditions. These are in fair agreement with the observed values of 1.1 and 0.25 n_c seen in Fig. 1c, particularly when one considers the significant 2D effects operative in the ball experiment. For instance, the experimental geometry permits significant lateral flow of plasma, which tends to lessen the resultant super-critical density jump. Experiments at similar intensity but with the probe pulse delayed several hundred psec showed no density jump near critical. The measured profile steepening during peak irradiation therefore tends to confirm the essential role of radiation pressure in these experiments. For completeness it is worth noting that on a shot to shot basis in these experiments the lower shelf density varied considerably more than that of the upper shelf, e.g., from 0.2 to 0.5 as compared to 1.0 to 1.2 n_c for the upper shelf. In experiments with intensities as low as 10^{13} W/cm^2 a slight density jump was discernable, in qualitative agreement with the early theoretical work.[11] Higher intensity experiments, to 3 x 10^{15} W/cm^2, have recently been performed using an f/1 focusing lens. Interpretation is not yet complete, the significant issue being that of fringe loss due to a large density step.

Further evidence supporting the role of radiation pressure has been obtained in our experiments with flat disk targets. Fig. 2a shows an interferogram of a 70 μm diameter, 1 μm thick tungsten glass disk, approximately 10 psec after a peak intensity of 3 x 10^{14} W/cm^2. General features of the fringe pattern permit one to make several interesting observations without recourse to numerical inversion. For instance, the fact that the inner fringes run parallel to the original target surface, rather than bowing out, is clear evidence of a large scale density hole or cavity on axis. In addition, fluctations in the fringe pattern are strongly correlated with fluctuations of electron density so that one can readily infer density variations of

20% amplitude and 5-7 μm scale size directly from Fig. 2a. Numerical inversion is possible and quantitative results are shown in Fig. 2b for a transverse plane 16 μm from the initial target surface. The pronounced density dip on axis is to be compared with the transverse profile of Fig. 1b for the ball target. Density cavities such as this were observed on all flat target experiments for intensities exceeding 10^{14} W/cm^2, but were not observed in experiments at 10^{13} W/cm^2, again supporting the significant role of radiation pressure in these experiments.

Additional factors observed with disk experiments include the fact that at equivalent intensity parylene disks generally display a larger degree of small scale rippling than the relatively smooth glass target of Fig. 2a. However, the 10^{13} W/cm^2 parylene disk experiments were relatively free of such effects as were all glass ball experiments. The observation of strong rippling in parylene disk experiments above 10^{14} W/cm^2 provides a valuable link between recent experimental and theoretical studies of angle dependent absorption at high intensity.[12].

In conclusion, we have presented well resolved electron density distributions which show clearly and directly the role of radiation pressure in plasmas produced by intense laser light. In sample results we see gradient steepening, quantitatively determined density jumps, cavity formation, and small scale rippling of the iso-density surfaces.

The authors acknowledge the excellent technical assistance of E. L. Pierce, and the encouragement and material support of their many colleagues in the Livermore Laser Fusion program, particulary C. E. Max, C. W. Hatcher, J. E. Swain, L. W. Coleman, H. G. Ahlstrom, and C. D. Hendricks.

REFERENCES

1. K. G. Estabrook, E. J. Valeo, and W. L. Kruer, Phys. Fluids 18, 1151 (1975); K. Lee, D. W. Forslund, J. M. Kindel, and E. L. Lindman, Phys. Fluids 20, 51 (1977).

2. E. J. Valeo and K. G. Estabrook, Phys. Rev. Lett. 34, 1008 (1975); K. G. Estabrook, Phys. Fluids 20, 51 (1977).

3. S. Jackel, B. Perry, and M. Lubin, Phys. Rev. Lett. 37, 95 (1976); D. W. Phillion, R. A. Lerche, V. C. Rupert, R. A. Haas, and M. J. Boyle, Phys. Fluids (in press).

4. T. P. Donaldson and I. J. Spalding, Phys. Rev. Lett. 36, 467 (1976); Yu. A. Zakharenkov, O.N. Krokhin, G. V. Sklizkov, and A. S. Shikanov, Sov. J. Quant. Elect. 6, 571 (1976); R. Fedosejevs, I.V. Tomov, and M. C. Richardson, Proc. XII Int'l. Congr. High Speed Photog., Toronto, Canada (1976).

5. F. W. Perkins and J. Flick, Phys. Fluids 14, 2012 (1971); C. S. Liu, M. N. Rosenbluth, and R. B. White, Phys. Fluids 17, 1211 (1974).

6. J. F. Holzrichter and D. R. Speck, J. Appl. Phys. 47, 2459 (1976).

7. V. W. Slivinsky, H. N. Kornblum, and H. D. Shay, J. Appl. Phys. 46, 1973 (1975).

8. D. T. Attwood, L. W. Coleman, and D. W. Sweeney, Appl. Phys. Lett. 26, 616 (1975); D. T. Attwood, Proc. XII Int'l. Congr. High Speed Photog., Toronto, Canada (1976); The primary advantages of this technique, in addition to providing the desired 1 μm resolution, are that it provides simple and accurate focusing, a necessary feature for strongly refracting media, and that it is relatively unaffected by harmonic emission from the plasma.

9. D. T. Attwood, E. L. Pierce, and L. W. Coleman, Optics Commun. 15, 10 (1975); D. T. Attwood, E. S. Bliss, E. L. Pierce, and L. W. Coleman, IEEE J. Quant. Elec. 12, 203 (1976).

10. D. W. Sweeney, D. T. Attwood, and L. W. Coleman. Appl. Optics 15, 1126 (1976).

11. R. E. Kidder, LLL UCRL-74040, 1972 (unpublished); K. J. Estabrook, E. Valeo, and W. L. Kruer Phys. Lett. 49A, 109 (1974).

12. K. R. Manes, V. C. Rupert, J. M. Auerbach, P. H. Y. Lee, and J. E. Swain, Phys. Rev. Lett. 39, 281 (1977); J. J. Thomson, W. L. Kruer, A. B. Langdon, C. E. Max, and W. C. Mead (to be published).

FIGURE CAPTIONS

Figure 1. (a) Interferogram at peak irradiation of a 41 μm diameter ball. $I \simeq 3 \times 10^{14}$ W/cm^2. (b) Transverse electron density profile at an axial position 4 μm from the initial target wall. (c) Density profile on axis demonstrating steepening due to radiation pressure. Solid lines are best fit; e-folding scale lengths ℓ_u, ℓ_c, and ℓ_ℓ are indicated for the upper, critical, and lower density regions. Typical error bars are shown in (b) and (c); $n_c = 10^{21}$ e/cc.

Figure 2. (a) Interferogram of a 70 μm diameter glass disk approximately 10 psec after peak irradiation intensity. $I \simeq 3 \times 10^{14}$ W/cm^2. (B) *Transverse profile at an axial* position 16 μm from the initial target wall. Note the pronounced density cavity and compare with Fig. 1b. Typical error bars are displayed.

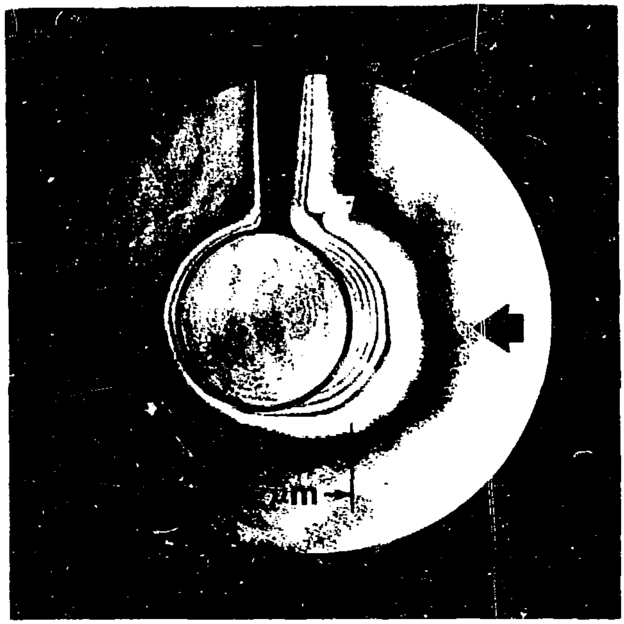

FIGURE 1a

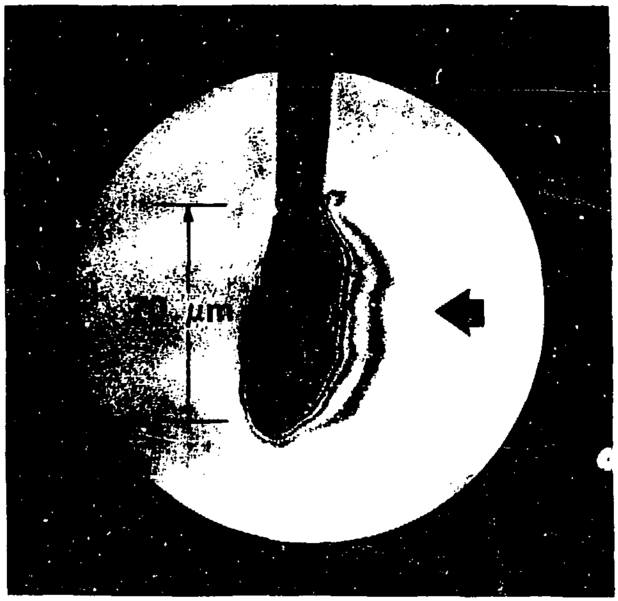

FIGURE 2a

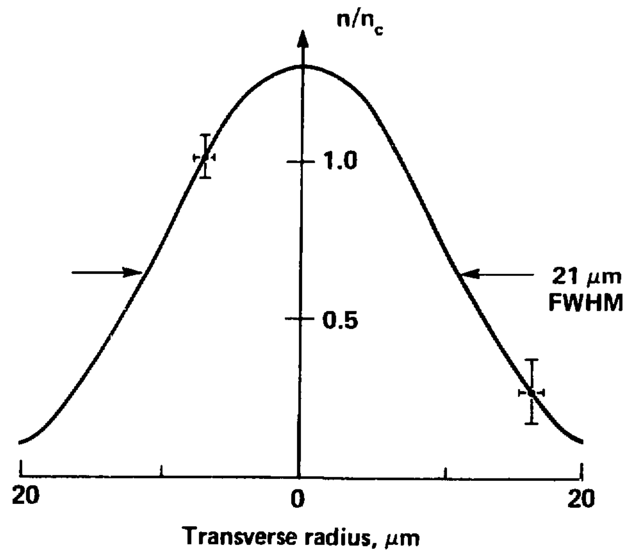

FIGURE 1b

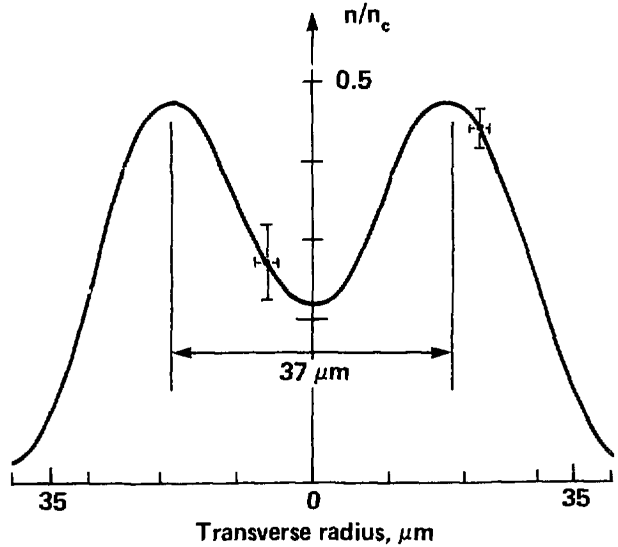

FIGURE 2b

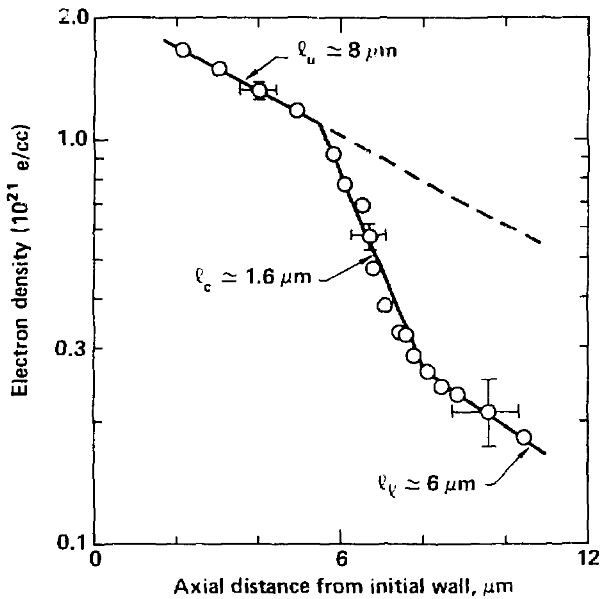

Electron density (10^21 e/cc)
2.0
1.0
0.3
0.1
ℓu ≃ 8 μm
ℓc ≃ 1.6 μm
ℓℓ ≃ 6 μm
0
6
12
Axial distance from initial wall, μm

FIGURE 1c